

EXCLUSIVE DEEPLY INELASTIC ELECTROPRODUCTION AT HERMES

J. LU, ON BEHALF OF THE HERMES COLLABORATION

TRIUMF, 4004 Wesbrook Mall, Vancouver, Canada
E-mail: jiansen@triumf.ca

Asymmetries in beam charge, beam helicity and target polarization have been measured for hard exclusive electroproduction of photons, ρ^0 and π^+ in HERMES. The asymmetries appear in the distribution of the photons or mesons in the azimuthal angle around the virtual photon direction, relative to the lepton scattering plane. Such asymmetries can constrain the Generalized Parton Distributions (GPDs) of the nucleon or nucleus. The experiment is performed at the DESY laboratory in Hamburg Germany, using 27.5 GeV positrons and electrons incident on hydrogen, deuterium and neon targets.

1. Introduction and motivation

Hard exclusive meson electroproduction and Deeply Virtual Compton Scattering (DVCS) have provided several experimental constraints on the off-forward behavior of the Generalized Parton Distributions (GPDs), which contain information on two-parton correlations, quark transverse spatial distributions and orbital angular momentum distributions^{1,2,3,4,5}. DVCS is the hard exclusive electroproduction of a real photon, in which a quark absorbs a hard virtual photon, re-emits an energetic real photon and then rejoins the target remnant to leave the target nucleon intact. DVCS is the cleanest process in which the GPDs can be measured. At moderate lepton beam energies, the DVCS process can not be separated from the more abundant Bethe-Heitler (BH) process because of the identical final state. However the DVCS amplitudes can be studied through asymmetries that arise from the interference between these two processes. The interference term in the cross section depends on the charge and helicity of the incident lepton and the polarization of the target. This gives rise to asymmetries in either beam charge, beam helicity or target polarization appearing in the distribution of the photon in the azimuthal angle ϕ around the virtual photon direction, relative to the lepton scattering plane^{6,7,8}. The interference

term $\sigma_{\mathcal{I}}$ can be expanded in a Fourier series in the azimuthal angle ϕ :

$$\sigma_{\mathcal{I}} \propto c_0^{\mathcal{I}} + \sum_{n=1}^3 [c_n^{\mathcal{I}} \cos(n\phi) + s_n^{\mathcal{I}} \sin(n\phi)], \quad (1)$$

where $c_0^{\mathcal{I}}$, $c_n^{\mathcal{I}}$ and $s_n^{\mathcal{I}}$ can be expressed as linear combinations of nucleon or nuclear Compton Form Factors (CFFs) ⁹. They depend on the beam charge, beam helicity and target polarization. The CFFs can be expressed as convolutions of the leading-order hard-scattering vertex with the GPDs. Significant azimuthal beam spin and beam charge asymmetries in hard electroproduction of photons on a hydrogen target have been reported in Refs. ^{10,11,12}.

At leading twist, there are four GPDs appear in the description of DVCS in the nucleon, $H(x, \xi, t)$, $E(x, \xi, t)$, $\tilde{H}(x, \xi, t)$ and $\tilde{E}(x, \xi, t)$, related to the vector, tensor, axial-vector and pseudoscalar transitions, where x is the quark longitudinal momentum fraction, ξ is the difference of longitudinal momentum fraction between the absorbing and emitting quarks and t is the squared four momentum transfer between initial and final nucleon.

Recently, measurements of azimuthal asymmetries for DVCS on nuclear targets have been recognized as a useful source of information about partonic behavior in nuclei and nuclear binding forces ¹³. Chiral symmetry can be restored in nuclear matter and the vector meson mass may be changed in nuclear matter. Studying DVCS on nuclei may shed light on this.

DVCS measures the GPDs on the line $x=\pm\xi$. In order to go off $x=\pm\xi$, all kinds of exclusive reactions are needed to constrain GPD models.

Using \uparrow and \downarrow to denote the positive and negative beam helicities and $\uparrow\uparrow$ and $\downarrow\downarrow$ to denote the target spin anti-parallel and parallel to the beam momentum direction in the target rest frame, a beam spin asymmetry $A_{LU}(\phi)$ in the cross section of a polarized beam on an unpolarized target can be written as:

$$A_{LU}(\phi) = \frac{d^{\uparrow}\sigma(\phi) - d^{\downarrow}\sigma(\phi)}{d^{\uparrow}\sigma(\phi) + d^{\downarrow}\sigma(\phi)}. \quad (2)$$

The longitudinally polarized target spin asymmetry with an unpolarized beam can be written as:

$$A_{UL}(\phi) = \frac{d^{\uparrow\uparrow}\sigma(\phi) - d^{\downarrow\downarrow}\sigma(\phi)}{d^{\uparrow\uparrow}\sigma(\phi) + d^{\downarrow\downarrow}\sigma(\phi)}. \quad (3)$$

The beam charge asymmetry for unpolarized beam scattering from an

unpolarized target can be written as:

$$A_{CU}(\phi) = \frac{d^+\sigma(\phi) - d^-\sigma(\phi)}{d^+\sigma(\phi) + d^-\sigma(\phi)}, \quad (4)$$

where $+$ and $-$ represent positron and electron beams.

At the twist-two level, $A_{LU}(\phi)$ and $A_{UL}(\phi)$ have a $\sin \phi$ dependence and $A_{CU}(\phi)$ has a $\cos \phi$ dependence.

2. The HERMES detector

A full description of the HERMES detector can be found elsewhere¹⁴ and only those components relevant for this analysis are described here. A longitudinal polarized positron/electron beam of 27.6 GeV from the HERA storage ring at DESY is used to scatter off internal gas targets. In the HERA storage ring, the positrons are naturally transversely polarized by the emission of synchrotron radiation – the so called ‘Sokolov-Ternov effect’¹⁵. The transverse beam polarization is transformed locally into longitudinal polarization by a spin-rotator¹⁶ before entering the experiment and is rotated back by an spin-rotator after the experiment. The sign of the beam polarization is changed about every two months.

The scattered positrons or electrons and produced particles are detected by the HERMES spectrometer¹⁴ in the range $0.04 \text{ rad} < \theta < 0.22 \text{ rad}$ of the polar angle. Charged particle identification is accomplished using four detectors: a Čerenkov counter, a transition-radiation detector, a preshower scintillator counter and a lead-glass calorimeter. The average positron identification efficiency is at least 98% with hadron contamination of less than 1%. Photons are identified by the detection of energy deposited in the calorimeter and preshower counter and by the requirement that there is no associated charged track seen in the drift chambers.

3. The DVCS measurements

The exclusive DVCS events were selected via missing mass. The missing mass squared for a proton target is defined as: $M_X^2 = (q + P_i - P_\gamma)^2$, where q , P_i and P_γ are the four-momenta of the virtual photon, the initial target nucleon and the produced real photon. Due to the finite momentum resolution of the spectrometer and the calorimeter, M_X^2 may be negative. ‘Exclusive’ events were selected in $-2.25 \text{ GeV}^2 < M_X^2 < 2.89 \text{ GeV}^2$ to minimize the DIS-fragmentation background while optimizing the statistics. For nuclei, M_X^2 is calculated based on the initial target mass as a proton

mass and the same restriction $-2.25 \text{ GeV}^2 < M_X^2 < 2.89 \text{ GeV}^2$ is applied, resulting in most exclusive events still being selected.

The DVCS beam spin asymmetry on the proton was published in ¹⁰. The DVCS beam spin asymmetry on the deuteron and neon *vs* azimuthal angle ϕ are shown in Fig. 1. The incoherent process dominates for the deuteron and the main contribution is from the proton, while the coherent process dominates for the neon target.

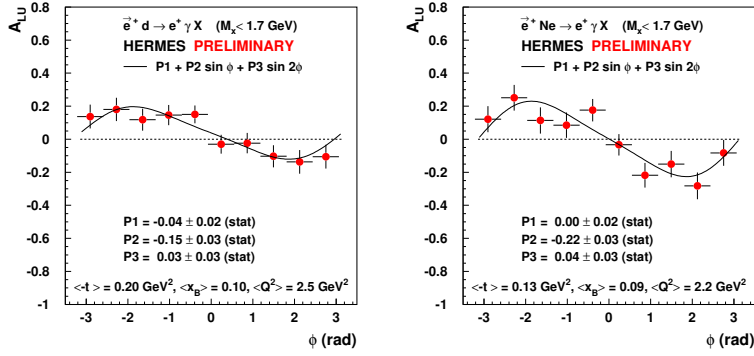


Figure 1. The DVCS beam spin asymmetry vs azimuthal angle ϕ on deuterium (left) and neon (right) target.

The target spin asymmetry on the deuteron vs azimuthal angle is shown in Fig. 2 (left).

The beam charge asymmetry on the proton vs azimuthal angle ϕ are shown in Fig. 2 (right). The dashed and dashed-dotted lines in Fig. 2 (right) are based on the chiral quark soliton model calculated at twist-2 and twist-3 levels including the D-term contribution ¹⁷. The dotted line is twist-2 without D-term. The long-spaced dashed line is twist-2 with the reverse sign for the D-term. The HERMES data favor the existence of the D-term contributions, the D-term sign can be determined.

4. Exclusive production of ρ^0 and π^+

There are two Feynman diagrams for exclusive meson production, which are two gluon exchange and quark exchange diagrams. They are shown in Fig. 3.

The ρ^0 is identified by its decay $\rho^0 \rightarrow \pi^+ \pi^-$. The exclusive events are

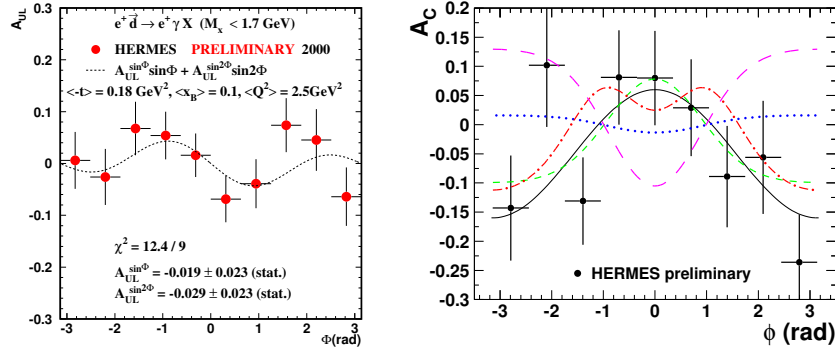


Figure 2. The DVCS target spin asymmetry on deuteron *vs* azimuthal angle ϕ (left) and the DVCS beam charge asymmetry on proton *vs* azimuthal angle (right). The solid line in the right plot represents $P_1 + P_2 \cos \phi$ fit. The other curves are model calculations described in the text.

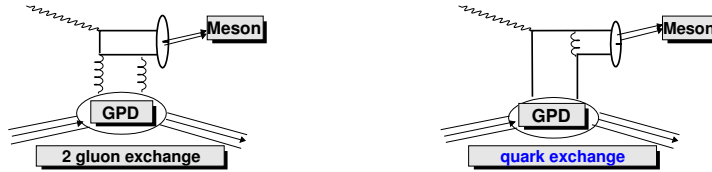


Figure 3. Leading twist diagrams for hard exclusive reactions.

selected by using $\Delta E < 0.4 \text{ GeV}$, where $\Delta E = (M_X^2 - M_p^2)/(2M_p)$. Here M_p is the proton mass and P_{ρ^0} is the four-momentum of the produced ρ^0 meson. As the factorization theorem applies only to the longitudinal photons, the decay angular distribution is used to select the contribution from longitudinal photon. The longitudinal component of the ρ^0 virtual-photon production cross-section *vs* W for $\langle Q^2 \rangle = 2.3 \text{ GeV}^2$ and $\langle Q^2 \rangle = 4.0 \text{ GeV}^2$ are shown in Fig. 4, where W is the photon-nucleon invariant mass. The calculation results of M. Vanderhaeghen¹⁹ are also shown in Fig. 4.

Target Spin asymmetries for exclusive ρ^0 production on the deuteron and for the π^+ on the proton are shown in Fig. 5. A significant $\sin \phi$ target spin asymmetry is measured for exclusive π^+ production on proton target,

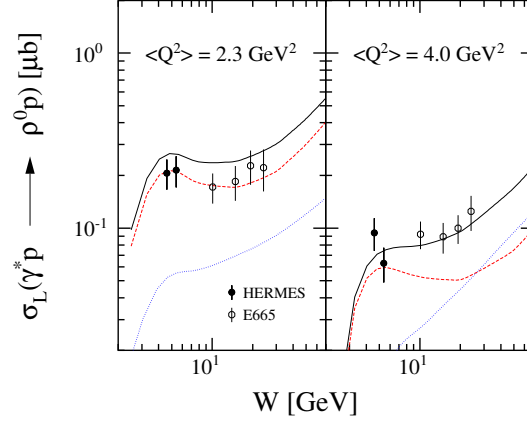


Figure 4. The longitudinal component of the virtual-photon production cross-section for ρ^0 production vs W (bottom). The solid lines represent the calculation results of M. Vanderhaeghen. The dashed (dotted) curves represent the quark (two-gluon) exchange contributions within these calculations.

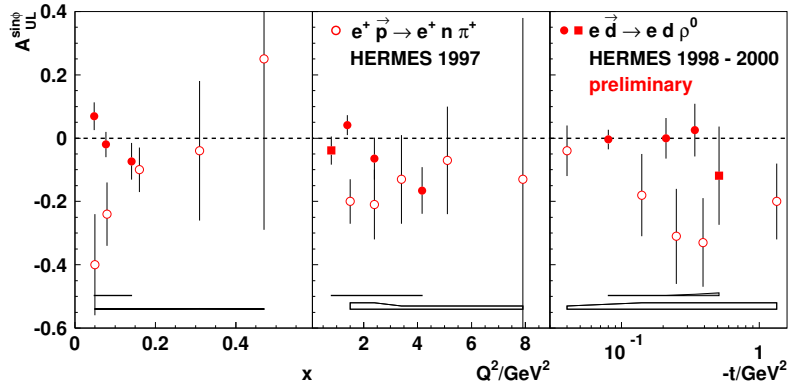


Figure 5. Kinematic dependence of the target spin asymmetry $A_{UL}^{\sin \phi}$ for exclusive π^+ production on the proton and ρ^0 production on the deuteron. The full squares indicate data points outside the integration limits of the kinematic variables used for the overall asymmetry.

while the $\sin \phi$ target spin asymmetry for ρ^0 production on the deuteron is compatible with zero.

5. Conclusion

HERMES has measured the DVCS beam spin asymmetry on the proton, deuteron and on the neon, the target spin asymmetry on the deuteron, and the beam charge asymmetry on the proton. Exclusive production of ρ^0 and π^+ has been studied. HERMES is now recording proton data from a transversely polarized proton target. A recoil detector is being constructed for 2005-2007 to detect the recoil nucleon to select exclusive events in a cleaner way. Existing DVCS data can constrain GPDs²⁰.

References

1. X. D. Ji, Phys. Rev. Lett. **78**, 610 (1997).
2. M. Burkardt, AIP Conf. Proc. **588**, 199 (2001).
3. J. P. Ralston and B. Pire, Phys. Rev. D **66**, 111501 (2002).
4. M. Diehl, Eur. Phys. J. C **25**, 223 (2002).
5. A. V. Belitsky and D. Müller, Nucl. Phys. A **711**, 118 (2002).
6. M. Diehl, T. Gousset, B. Pire and J. P. Ralston, Phys. Lett. B **411**, 193 (1997).
7. A. V. Belitsky, D. Müller, L. Niedermeier and A. Schäfer, Nucl. Phys. B **593**, 289 (2001).
8. A. V. Belitsky, D. Müller and A. Kirchner, Nucl. Phys. B **629**, 323 (2002).
9. A. Kirchner and D. Müller, Eur. Phys. J. C **32**, 347 (2003).
10. HERMES Collaboration, A. Airapetian *et al.*, Phys. Rev. Lett. **87**, 182001 (2001).
11. F. Ellinghaus (for the HERMES Collaboration), Nucl. Phys. A **711**, 171 (2002).
12. CLAS Collaboration, S. Stepanyan *et al.*, Phys. Rev. Lett. **87**, 182002 (2001).
13. M. V. Polyakov, Phys. Lett. B **555**, 57 (2003), Eur. Phys. J. C **32**, 347 (2003).
14. HERMES Collaboration, K. Ackerstaff *et al.*, Nucl. Instrum. Methods A **417**, 230 (1998).
15. A. Sokolov and I. Ternov, Sov. Phys. Doklady **8**, 1203 (1964).
16. D.P. Barber *et al.*, Phys. Lett. B **343**, 436 (1995).
17. M. Radyushkin, Phys. Rev. D **59**, 014030 (1999).
18. A. Airapetian *et al.*, Eur. Phys. J. C **17**, 389-398 (2000).
19. M. Vanderhaeghen *et al.*, Phys. Rev. D **60**, 090417 (1999).
20. A. Freund, M. McDermott and M. Strikman, Phys. Rev. D **67**, 036001 (2003).